

# Spatial comparison of London's three waves of Spanish Flu

Walter Peterson

Captain, US Navy (Retired) Stafford, VA, USA

## Abstract

England and Wales experienced three waves of influenza during the 1918/19 Spanish Flu pandemic. A previous analysis showed that these three waves had fundamentally different spatial and temporal characteristics. This present study compares London's experience of the three waves to discern possible geographic differences on a metropolitan level. Borough mortality data for each wave were normalized and then scaled, with spatial autocorrelation techniques displayed by GIS software and analysed for each wave. Registrar General in England and Wales reporting provided data concerning measures of 'health' and 'wealth' for each metropolitan borough. Spearman's rank correlation determined the correlation of each wave's mortality to each of the other waves including the 'health,' 'wealth' and population density factors. The comparisons showed that there is a spatial dif-

ference among the waves. The first two are spatially similar, with both exhibiting 'random' autocorrelation patterns, while the third wave exhibits a 'clustered' pattern. The borough mortality of the first two waves strongly correlated with each other, with both having similar 'health,' 'wealth' and population density factors. However, the third wave's mortality did not correlate with any of the first two and actually behaved in an opposite manner with regard to the 'health,' 'wealth,' and population density factors. These results do not appear in the literature and create new opportunities for research to explain London's mortality during the Spanish Flu pandemic of 1918/19.

## Introduction

The 1918/19 Spanish Flu pandemic has been described as one of the deadliest events in recorded human history, killing an estimated 50-100 million persons (Morens & Fauci, 2007). In England and Wales, the toll was just over 150,000 (Registrar General, 1920). The epidemic devastated London in three waves from June of 1918 through May of 1919. Over 17,000 Londoners succumbed at a death rate of nearly five per 1,000 of civilian population due to the influenza virus. A team of geographers from the Universities of Cambridge and Nottingham studied, on the national level, the spatial characteristics of the epidemic (Smallman-Raynor *et al.*, 2002) showing that the three waves each exhibited differing geographic characteristics.

This study compares spatially and statistically each wave to each of the other two based on geographic mortality distributions, autocorrelation patterns, wave-weighted mean centres, and Spearman's correlation coefficients, thereby determining the existence of differing geographic patterns on the metropolitan level. The Registrar General Weekly Reports (hereafter identified as RGWR, year) provide location information for the weekly death counts. The Supplement to the Eighty-First Annual Report of the Registrar-General of the Births, Deaths and Marriages in England and Wales (hereafter referred to as Registrar-General, 1920) provides summary statistics for the administrative units of England and Wales and published measures of 'health' in the form of a standardized death rate for 1911-14 and of 'wealth' in the form of the percentage of the 1911 population employing domestic indoor servants for each of London's 29 boroughs. Normalizing death count data provided the basis for comparing the mortality of the borough waves. The RGWR (1919) supplies the borough population estimates used in the normalization process. These estimates refer to the year 1917 as the best available at the time. The process concluded with a 0 to 1 scaling of the normalized results. Mapped wave scaled data allowed for wave visual inspection and comparison. Analyses of quantile-quantile plots confirmed that all the datasets compared were not normally distributed.

Correspondence: Walter Peterson, Captain, US Navy (Retired), 2266 Aquia Drive, Stafford, VA, 22554, USA.  
E-mail: wpete3bx@mail.umw.edu

Key words: London Spanish Flu; influenza wave comparison; GIS applications.

Conflict of interest: the authors declares no potential conflict of interest, and all authors confirm accuracy.

Availability of data and materials: all data generated or analyzed during this study are included in this published article.

Acknowledgement: the author expresses appreciation to Professor Debra Hydorn (Department of Mathematics, University of Mary Washington, Fredericksburg, VA, USA) for valuable insights in statistical analysis.

Received: 7 August 2023.  
Accepted: 4 December 2023.

©Copyright: the Author(s), 2023  
Licensee PAGEPress, Italy  
Geospatial Health 2023; 18:1235  
doi:10.4081/gh.2023.1235

This work is licensed under a Creative Commons Attribution-NonCommercial 4.0 International License (CC BY-NC 4.0)

Publisher's note: all claims expressed in this article are solely those of the authors and do not necessarily represent those of their affiliated organizations, or those of the publisher, the editors and the reviewers. Any product that may be evaluated in this article or claim that may be made by its manufacturer is not guaranteed or endorsed by the publisher.

## Materials and Methods

### Study area

London County constitutes the study area. The *London Government Act of 1899* (Terry & Morle, 1899) established a system of 29 metropolitan boroughs. Although not technically classified as a borough, the Registrar-General mortality reporting treats the City of London as such. Figure 1 shows the outlines of the boroughs and highlights the City of London for a visual orientation aid. Figures 2 and 3 show the study area's relevant characteristics. Figure 2 shows the distribution of the 'health' and 'wealth' indices

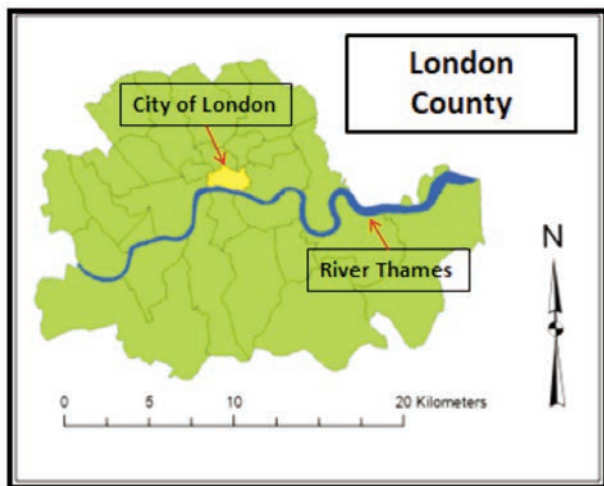


**Figure 1.** London County is the area studied. Shown are the outlines of the Metropolitan Boroughs and the City of London (highlighted for orientation purposes) that make up the 29 mortality reporting locales.

published by the Registrar-General in 1920 for each borough. Figure 3 displays 1919 borough population densities.

### Data sources

The main data sources have been identified in the introduction. The RGWRs provided weekly mortality data and Registrar-General (1920) the borough 'health' and 'wealth' data. Borough acreage data are from Vision of Britain ([https://visionofbritain.org.uk/census/table/EW1961COU\\_M3?u\\_id=10041790&show=D&min\\_c=1&max\\_c=12](https://visionofbritain.org.uk/census/table/EW1961COU_M3?u_id=10041790&show=D&min_c=1&max_c=12)). The *London Government Act of 1899* provided the basis for creating the geographical information systems (GIS) portraying the 29 boroughs of London as they were constituted during the pandemic.

### Notes on the data

Registrar-General (1920) presents several methods to overcome an expected under-reporting of the epidemic's mortality due to allocation of some deaths to other causes that rightfully should be attributed to influenza. Registrar-General (1920) states that "... none of them [is] wholly satisfactory..." (Registrar-General, 1920, p. 3). Consequently, and because the mortality data were used in a comparative manner, this study used the borough mortality statistics and wave timing as tabulated in the supplement without alteration.

The borough acreage values used are from the 1961 census report contained in Vision of Britain. This is the last census before the 1965 supersession of the borough organization established by the *London Government Act of 1899*. The acreage in the 1961 listing is imagined to be more precise than the 1911 and 1921 listings. Interestingly though, no borough had a difference among the three census listings approaching 1%.

### Data processing

The software package ArcGIS Pro software (ESRI, Redlands, CA, USA) was used to display and spatially analyse the borough mortality data and Spearman's rank correlation coefficient calculations were used to compare the distributions of influenza deaths for

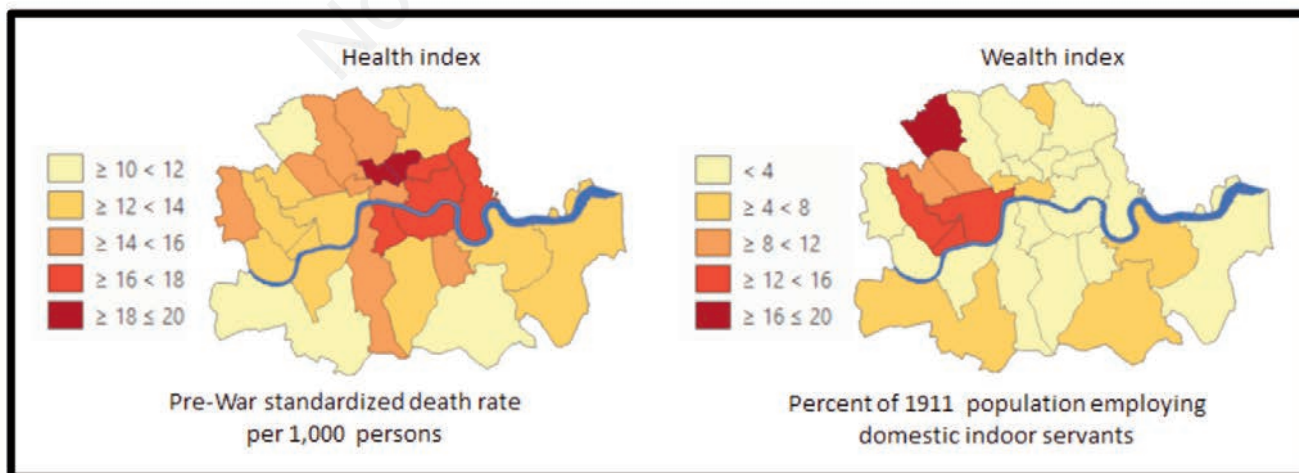


**Figure 2.** The Registrar-General published in 1920 indices of 'health' and 'wealth' for each of the Metropolitan Boroughs. The 'health' index' reported the pre-war standardized death rate per 1,000 persons. The 'wealth' index reflected the percentage of the 1911 population employing domestic indoor servants.

each borough among the waves. ArcGIS Pro (3.1.2) determined a weighted mean centre for each wave. This can be thought of as the wave's centre of 'mortality' and was used for comparison with the other waves. Moran's  $I$  determined a global autocorrelation coefficient for comparing the mortality among neighbouring boroughs throughout the London study area for each wave. The algorithm evaluated whether the mortality pattern was clustered, dispersed or random and provided a  $z$ -score and a  $p$ -value to aid the determination of whether or not to reject a null hypothesis that would indicate a randomly distributed pattern (*i.e.* spatially uncorrelated).

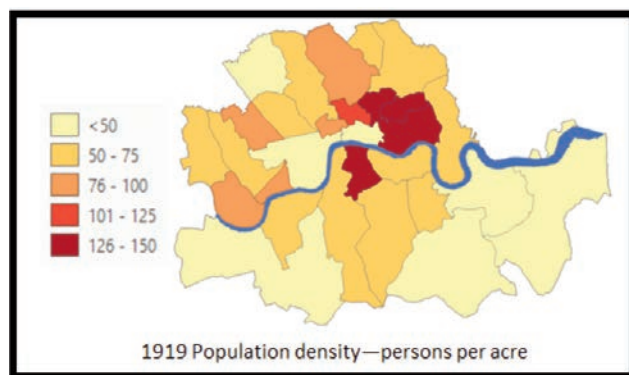


**Figure 3.** Borough population density displayed in persons per acre. The Registrar-General determined in 1919 that the 1917 population estimates were the best available at the time and are the estimates used in this density depiction.

## Results

London experienced the first of three Spanish Flu waves from the week ending 23 June 1918 through the week ending 14 September. This wave proved to be the mildest of the three, with 997 dying of the flu. The second wave continued from 15 September 1918 through 25 January 1919. It proved to be the most virulent on, killing 12,330 Londoners. The third and final wave ran from 26 January to 10 May 1919. It was not as deadly as the second but more than the first wave, leaving 3,786 dead in the Metropolis. The vastly differing mortality among the waves required an unusual data grouping to display the normalized and scaled data for a meaningful visual comparison. Figure 4 shows a side-by-side comparison of the waves' cumulative mortalities by borough. However, these unequal groupings played no role in subsequent Moran  $I$  or Spearman correlation calculations.

Table 1 shows the Moran  $I$  values for the three waves. Given the  $Z$  scores and  $p$ -values of waves 1 and 2, their patterns presented as random patterns. The third wave's  $Z$  score of 3.470251, on the other hand, gave less than 1% likelihood that the clustered pattern could be the result of random chance. Significant here is that waves 1 and 2 shared the same 'random' pattern type across the study area, while the 3<sup>rd</sup> wave presented as a 'clustered' pattern type. Figure 5 shows the relative locations of the three waves' centres weighted by their respective boroughs' wave total mortality. The centres of the first and second waves were relatively close together, while that of the third was located 0.8 km to the west of the first two.

Tables 2 and 3 show the results of Spearman's rank correlation coefficient comparisons. Table 2 displays wave to wave borough mortality comparisons and Table 3 the results of comparing each wave with the indices of population density, pre-war borough standardized death rate, and a 'wealth' index reflecting the percentage of borough population employing live-in domestic help.

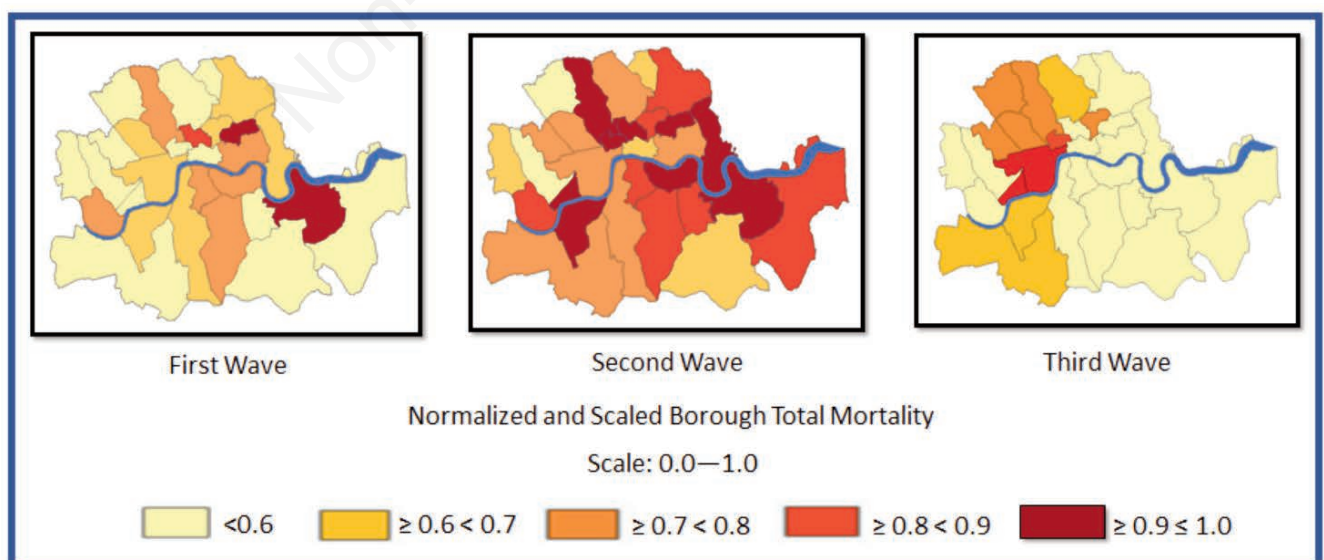


**Figure 4.** Side-by-side comparison of each wave's borough total mortality. The data has been normalized and scaled. The significant differences in wave mortality have necessitated the unusual scale groupings to allow a meaningful visual comparison.

Conceptually, these datasets represent the entirety of a population, not a sample from a larger population. Consequently, with no sampling variability to account for, assigning a  $p$ -value to the correlation coefficient ( $r_s$ ) would be meaningless. The Registrar-General expressed concern that "...during influenza epidemics the mortality attributed to the disease does not represent the whole of that

caused by it" (Registrar-General, 1920, p.3). Because of this concern, the datasets were treated as 'samples' from the larger population of 'all Spanish Flu mortality' and a  $p$ -value calculated as seen in Tables 2 and 3. The similarity of waves 1 and 2 correlation coefficients, not only with each other but also with the health, wealth, and population density factors is noteworthy. Importantly, wave 3 was not similar to waves 1 and 2 in any case; in some cases even being opposite in direction.

The overall results indicate that the third wave both spatially and statistically varied from the preceding two waves, with its 'clustered' autocorrelation pattern differing from the 'random' autocorrelation patterns of waves 1 and 2. The Spearman correlation coefficients comparing the borough mortality of wave 1 with wave 2 showed strong correlation, while wave 3 neither correlated with wave 1 nor with wave 2. Wave 1 and 2 mortalities demonstrated moderate to strong correlation with the health, wealth, and population density indices, while wave 3 only demonstrated very weak correlations.

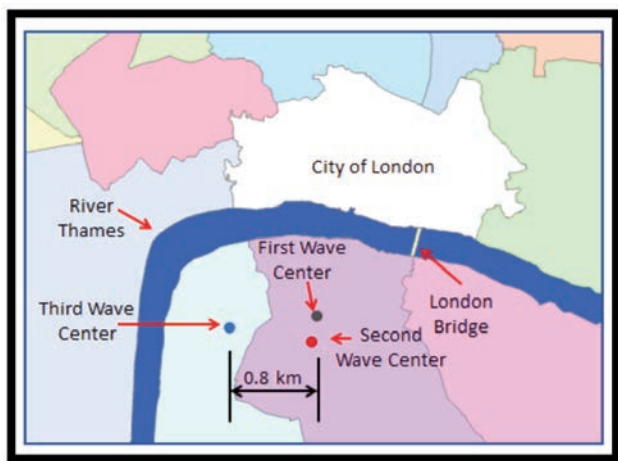


Figure 5. The geographic centre of each wave has been weighted by the wave's total mortality and is shown in relation to each other.

Table 1. Moran indices for the three waves.

Wave	Moran's $I$	Z	P
1	-0.012001 (random)	0.184549	0.853583
2	0.022641 (random)	0.449361	0.653172
3	0.405141 (clustered)	3.470251	0.000520

Table 2. Wave vs. wave Spearman coefficients.

Waves Compared	$r_s$	p-value
w1:w2	0.60889	0.0004563
w1:w3	-0.22815	0.2339143
w2:w3	0.00470	0.9807023

Table 3. Wave vs. index Spearman coefficients.

Wave	Health	Wealth	Pop. Density
1	$r_s = 0.51409$ $p = 0.00433$	$r_s = -0.59747$ $p = 0.00062$	$r_s = 0.45121$ $p = 0.01402$
2	$r_s = 0.49747$ $p = 0.00604$	$r_s = -0.60306$ $p = 0.00053$	$r_s = 0.42801$ $p = 0.02055$
3	$r_s = -0.17666$ $p = 0.35928$	$r_s = 0.35598$ $p = 0.05805$	$r_s = 0.11265$ $p = 0.56070$

## Discussion

An initial, simple visual inspection and comparison of the waves' mortality patterns in Figure 4 shows the third wave's mortality predominately to the west and north-west within London County rather than spread about as in the first two waves. The Moran's  $I$  analysis and comparison confirms this visual impression by showing that the first two waves had 'random' patterns and the third wave a 'clustered' pattern. The third wave's Moran's  $I$  of 0.405141 and  $Z$  of 3.470251 at  $p=0.000520$  shows the wave's 'global' clustering to be significant across the study area. The comparison of the waves' mean-weighted centres supports, although weakly, a third wave difference, whereas the centres of waves 1 and 2 almost coincide, with the third wave's centre markedly to the west of them by almost a kilometre.

As with the Moran  $I$  comparisons the resultant Spearman correlation coefficients present a strong case for the third wave being conspicuously different from the preceding two. Despite undoubted borough population fluctuations between the waves affecting their absolute precision, the similarities between waves 1 and 2 and their dissimilarity with wave 3 are overwhelming when using the calculated coefficients in a comparative manner. With a coefficient of 0.60889 and a  $p$ -value of 0.00045629, wave 1's borough mortality correlation with wave 2's borough mortality is strong while neither wave 1 nor 2 noticeably correlated with wave 3. While the correlation coefficients of waves 1 and 2 associated equally well with the indices of health, wealth, and population density, wave 3's correlation with these indices, differed significantly from those characterizing wave 1 and 2 in each case.

Beyond simply noting that the third wave statistically differed from the first two, the actual nature (sign) of the correlations investigated becomes extremely interesting, because it is counterintuitive. The first two waves' correlation coefficients, with respect to 'health', 'wealth' and population density, turned out to be within 0.03 of each other indicating a positive relationship with 'health' and population density and a negative relationship with 'wealth'. In other words, the increasing 'health' index denoted an increasing mortality and the increasing population density denoted an increasing mortality, while the increasing wealth index denoted a decreasing mortality. The nature (signs) of the third wave's coefficients, on the other hand differed in two important cases from waves 1 and

2. It showed a negative coefficient with the 'health' index, which has the inference that an increase in the 'health' index decreases the mortality. However, this wave also had a positive coefficient with the 'wealth' index and population density index denoting that increasing mortality is associated with increasing wealth and increasing population density. The relevant observation being that not only was the third wave opposite from wave 1 and 2 regarding its relationship with the 'health' and 'wealth' indices, it also indicated a shift in the socioeconomic class most at risk.

---

## Conclusions

The current literature does not document the spatial dissimilarity of London's third wave of the Spanish Flu from the other two. This study's spatial and statistical results do so, but do not point to a cause. Nevertheless, it is noteworthy that the first and second waves correlated with each other and that each correlates with the notion that the 'socially disadvantaged,' living in dense population circumstances, are the 'unhealthiest' and are subject to the greatest risk during this pandemic, a fact that might be repeated in the future. Importantly, however, the third wave upsets that notion of the wealthiest living in more 'luxurious' and usually healthier conditions, as they actually experienced a higher mortality.

Why did the third wave behave counterintuitively—especially after two waves that followed the expected paradigm? Was it in some way related to the war transitioning from endless trench warfare to an armistice and finally peace while experiencing at first a trickle and later an ever increasing flood of infected, returning servicemen? This of course is a rhetorical question. But the question of 'why the difference' is not. It also is a timely question during the era of COVID and its variants.

Within the realm of geographic information science and its tools, this study has shown areas worthy of further research and exploration, specifically detailed analysis of each wave as opposed to the 'global' analysis of this study. This study's results also provide valuable input to epidemiologists and demographers as they build and test models to explain the wave nature of flu epidemics with application to a better understanding of the wave nature of the current COVID pandemic. The ultimate goal is of course the hope of more rapid identification and mitigation of the next pandemic.

---

## References

- Morens D, Fauci A, 2007. The 1918 Influenza Pandemic: Insights for the 21<sup>st</sup> Century. *J Infect Dis* 195:1018-28.
- Registrar-General, UK. 1919. *Weekly Return of Births and Deaths Registered: London and Ninety-Five Other Great Towns (Vol. LXXX, 1919)*. His Majesty's Stationary Office, London, 847.
- Registrar-General, UK. 1920. *Report on the mortality from influenza in England and Wales during the epidemic of 1918-19: Supplement to the Eighty-First Annual Report of the Registrar-General of Births, Deaths, and Marriages in England and Wales*. His Majesty's Stationary Office, London, 119 pp.
- Smallman-Raynor M, Johnson N, Cliff A, 2002. The spatial anatomy of an epidemic: influenza in London and the county boroughs of England and Wales, 1918-1919. *Trans Instit Brit Geogr* 27:452-470.
- Terry G, Morle P, 1899. *The London Government Act 1899: with Explanatory Notes Embodying the Incorporated Enactments, with an Introduction and Index*. London: Butterworth & Co, 237 pp.